QUANTITATIVE MORPHOLOGICAL ANALYSIS OF CARBON BLACK IN POLYMERS USED IN LASER TRANSMISSION WELDING






C.Y. Wang[1] P.J. Bates[2] M. Aghamirian[3] G. Zak[4] R. Nicholls[4] M. Chen[4]

[1] Soochow University, Suzhou (P.R. China)
[2] Royal Military College, Kingston (Canada)
[3] Kingston Process Metallurgy Inc., Kingston (Canada)
[4] Queen's University, Kingston (Canada)

ABSTRACT

In laser transmission welding of thermoplastics, carbon black (CB) is often used to absorb laser energy and to convert it into heat. This process is controlled by the level and dimensions of the CB dispersed in the absorbing polymer. This study presents a technique for quantifying the CB morphology in polyamide 6 (PA6) and polycarbonate (PC) used in laser welding applications. The microstructure of the CB was observed by transmission electron microscopy (TEM). The TEM photomicrographs of CB were quantitatively analyzed using an image processing technique. The microstructural parameters such as size, shape and distribution of CB particles and aggregates were obtained. The results show that number average aggregate diameter was 40 to 100 nm for the materials tested. The number average diameter of the particles making up the aggregates was in the range of 10-30 nm.

IIW-Thesaurus keywords: *Carbon; Imaging; Plastics; Quantitative analysis; Reference lists.*

1 INTRODUCTION

Laser Transmission Welding (LTW) technology has recently gained popularity due to its ability to join complex thermoplastic shapes with high strength welds, minimum flash, no relative part movement and little in the way of consumables [1-6]. In LTW, a laser-transparent and a laser-absorbent component are brought together under pressure. The laser energy is passed through the transparent material and absorbed by the absorbent material near the interface of the two parts. This energy is converted into heat, conducted into the transparent part, melting the interface and thus joining the two components upon cooling. Diode and Nd:YAG lasers with power from tens to hundreds of watts are used as laser light sources. Carbon black (CB), at levels of the order of 0.1 weight %, is the additive used in the laser-absorbent part to transform the laser energy into heat. The absorption coefficient in the laser-absorbent part is dependent on the CB concentration and size distribution [7-9]. However, no information exists regarding the CB morphologies in materials used in the LTW process. Chen *et al.* [8] have developed a technique for measuring the absorption coefficient in laser-absorbent parts as a function of CB concentration.

CB used in the laser transmission welding process consists of essentially spherical colloidal particles made up of concentric layers of graphite. These primary particles coalesce together to form aggregates, which are indivisible and rigid colloidal entities that are the smallest dispersible base unit. Depending on mixing process, aggregates are able to cluster together to form so-called agglomerates due to strong van der Waals forces [10].

Shape and size distribution of aggregates and particles in the absorbent part play a key role in light absorption

Doc. IIW-1780-06 (ex-doc. XVI-859-06) recommended for publication by Commission XVI "Polymer joining and adhesive technology".

and energy generation. Therefore, understanding the dispersion of CB is very important for further investigation of the laser light absorbing properties in the welding process. Significant research effort [11-17] has been spent characterizing CB used in rubber and elastomer-based applications. The CB level in these compounds is of the order of 20-40 weight %. The ASTM standard 3849 describes how this can be done on CB additives and on CB obtained from dissolved rubber compounds. No work has been found that describes a technique for measuring CB size distributions in solid state polymer at CB levels that are two orders of magnitude lower. The purpose of this research is to develop a technique for measuring CB microstructure in PC and PA6 and then performing preliminary quantitative characterizations of these materials.

2 EXPERIMENTAL

The polymers used in this study are AKULON F223-D BK223 polyamide 6 from DSM and Makrolon 2605-901510 polycarbonate from Bayer. These two materials are referred to as PA and PC respectively. Both contained 0.2 weight % CB. The source of the CB additive in these polymers is unknown. Ultra-thin sections (thickness of approximately 70 nm) were cut from polymer granules using an RMC Powertome X ultramicrotome. In addition, PC samples were dissolved in dichlomethane. A drop of solvent-polymer-CB slurry was placed on a carbon-coated 300 mesh copper grid and then dried for 5 minutes to create a thin film. The microstructures of the thin slices and the film were observed using a Hitachi H7000 transmission electron microscope (TEM) with an accelerating voltage of 75 KV.

3 IMAGE PROCESSING

The TEM photomicrographs of CB were quantitatively analyzed by using NIH (National Institute of Health) Image package using TIFF grayscale images.

The processing operation was divided into four steps, namely thresholding, smoothing, sharpening, and measurement. In order to count and measure the particles automatically, thresholding was applied to discriminate CB from surrounding background based on their gray values. Due to variations in film thickness and morphology, thesholding was carried out manually. All pixels equal to or greater than a single threshold level were displayed in black, and the other pixels were displayed in white. A smoothing operation was used to reduce isolated specks within the image by replacing the value of each pixel in the image by the weighted average of its 3×3 neighbours using a spatial convolution filter. The image was finally made sharper by increasing the contrast of pixels next to one another using a second 3×3 spatial convolution filter.

Aggregates in thresholded images were then automatically outlined, redrawn, counted and their dimensions measured. The two-dimensional projected area of the CB aggregate image, together with its perimeter were recorded. The number of aggregates (N_A), the area (A_i) and perimeter (P_i) of each aggregate were used in the calculations of other particle parameters discussed in the next section. N_A was 34, 37 and 112 for the PA, PC and dissolved PC respectively.

4 METHODS OF DISPERSION QUANTIFICATION

There are many ways of presenting the CB aggregate and particle size distributions, as well as aggregate shape information. This paper will use two such techniques: one described in ASTM 3849 [18] for rubber materials, and a simple fractal analysis that has previously been employed in the analysis of CB distributions in rubber [16-17].

4.1 ASTM 3849

An average characteristic diameter (d_i) for the small particles making up each aggregate was determined using the so-called mean chord length:

$$d_i = \alpha_i \, \pi \frac{A_i}{P_i} \tag{1}$$

where α_i is the aggregation factor used to correct for the fact that the mean chord on any aggregate is usually a measure of the average distance across multiple particles. It is given by:

$$\alpha_i = 13.092 \left(\frac{P_i^2}{A_i}\right)^{-0.92} \tag{2}$$

If this yields $\alpha_i < 0.4$ then a value of 0.4 is used. For the three different materials studied this value was approximately 0.8 ± 0.4.

The mean particle diameter (d_m) is given by:

$$d_m = \frac{\sum_{i=1}^{N_A} n_i \, d_i}{\sum_{i=1}^{N_A} n_i} \tag{3}$$

where

n_i is the number of the particles in each aggregate. It is computed as:

$$n_i = V_{Ai} / V_{Pi} \tag{4}$$

where

V_{Ai} and V_{Pi} are the aggregate and particle volumes respectively. The former is calculated using stereological principles, and the latter is determined from the spherical volume of the particles. They are given by the following equations:

$$V_{Ai} = \frac{8 \, A_i^2}{3 \, P_i} \tag{5}$$

$$V_{Pi} = \frac{\pi \, d_i^3}{6} \tag{6}$$

The weight mean particle diameter (d_w) is the ratio of the fourth to the third moment and is given by:

$$d_w = \frac{\sum_{i=1}^{N_A} n_i d_i^4}{\sum_{i=1}^{N_A} n_i d_i^3} \quad (7)$$

The particle diameter distribution can then be assessed by calculating its standard deviation or by calculating a particle size heterogeneity index (*hi*), which is the ratio of weight mean particle diameter to mean particle diameter similar to the polydispersity index used to assess polymer molecular weight distributions:

$$hi = \frac{d_w}{d_m} \quad (8)$$

The area-equivalent aggregate diameter is used to obtain a characteristic length (D_i) of each measured aggregate. It is calculated from the projected aggregate area using a circular model. The mean aggregate diameter (D_m), weight mean particle diameter (D_{wm}) and aggregate heterogeneity (*HI*) can also be calculated using equations similar to those found above.

$$D_i = (4A_i / \pi)^{1/2} \quad (9)$$

4.2 Fractal analysis

Fractal analysis is also used to quantify the shape of the CB aggregate [16, 17]. A fractal is an object that shows similar geometric features at all length scales [19]. They are often said to possess infinite detail. Examples in nature include ferns where each set of branches contains the same pattern but on a smaller scale. Simple two-dimensional objects in Euclidean space have integer dimensions – a line would have a dimension of 1 and a surface would have a dimension of 2. A complex fractal image such as a CB agglomerate can be described using a fractal dimension (D_f) between 1 and 2. The value of D_f can be used to assess the shape of the fractal. For CB aggregates, D_f ranges from 1.15 for ellipsoidal shapes to 1.32 for branched and star-like forms [17]. One peculiarity of fractals is that its perimeter (P_i) is related to the length scale or so-called yardstick (δ) used to measure it. As δ decreases, the P_i increases exponentially, and the fractal area (A_i) approaches a constant value. The relationship between P_i, D_f, δ and A_i is given by [19]:

$$P_i = C\delta^{(1-D_f)} A_i^{D_f/2} \quad (10)$$

where

C is a proportionality constant.

For a self-similar object, D_f is independent of δ. Therefore, the slope of a Log P_i versus Log A_i plot should yield a straight line whose slope is half the fractal dimension.

5 RESULTS AND DISCUSSION

5.1 ASTM 3849

Figures 1 to 3 illustrate typical TEM photomicrographs and processed images of CB in PA6, PC and dissolved PC respectively. In Figures 1 to 3, the black shapes and outlines of the TEM photomicrographs represent the CB aggregates. It shows that the aggregates in the microtomed PA6 and PC exhibit ellipsoidally shaped aggregates. The aggregate hetereogeneity index (Table 1) for both these materials is 1.5. This is slightly lower than

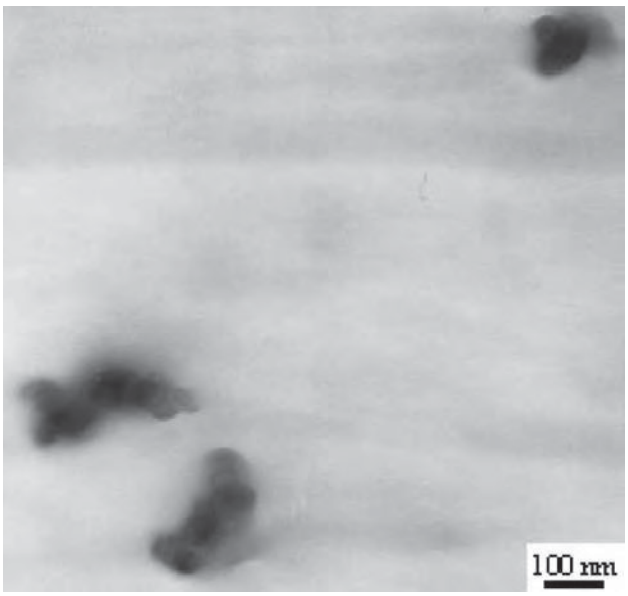

a) TEM photomicrograph of CB/PA6

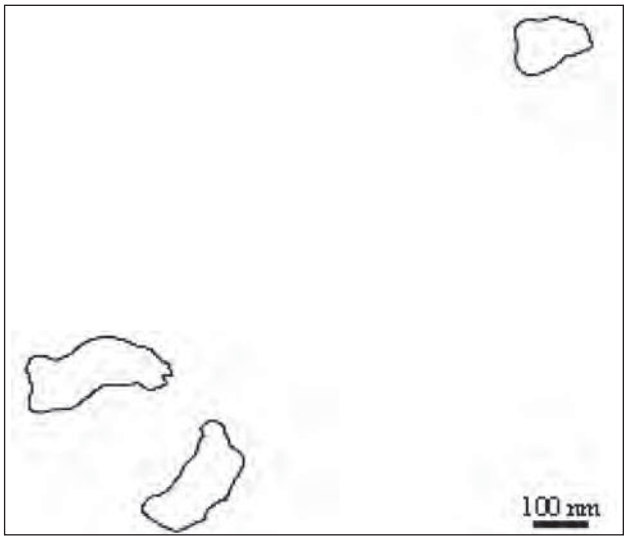

b) Same image after analysis

Figure 1

Table 1 – Particle and aggregate size of carbon black in PA6, PC and dissolved PC

Type	Particle Size				Aggregate Size			
	d (nm)	d_{wm} (nm)	s.d. (nm)	hi	D (nm)	D_{wm} (nm)	S.D. (nm)	HI
CB in Nylon6	32	51	15	1.6	96	147	48	1.5
CB in PC	13	17	4	1.3	38	55	16	1.5
CB Dissolved PC	13	18	5	1.4	61	190	47	3.1

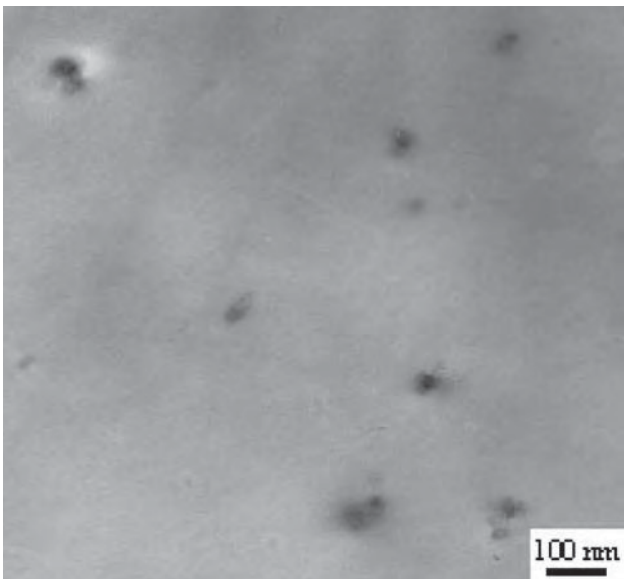

a) TEM photomicrograph of CB/PC

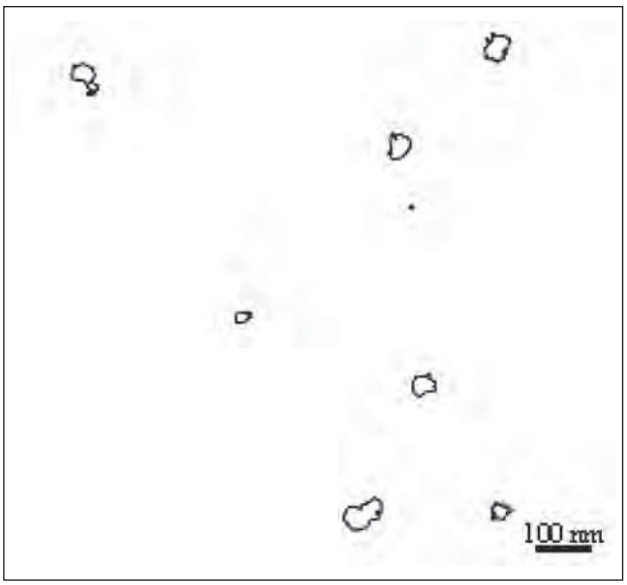

b) Same image after analysis

Figure 2

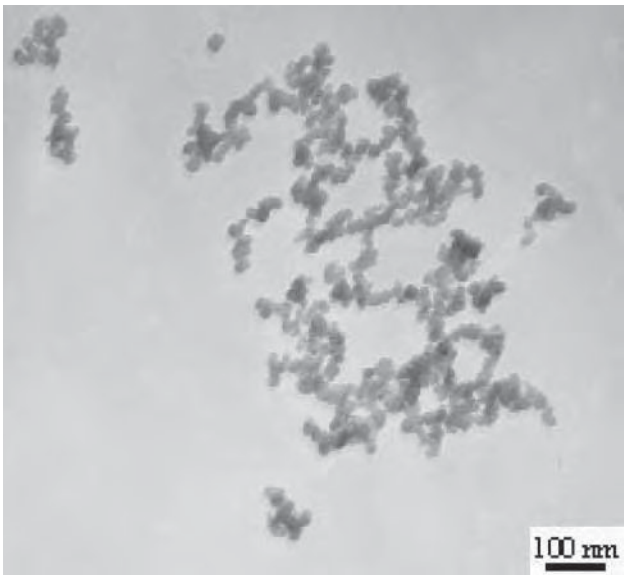

a) TEM photomicrograph of dissolved CB/PC

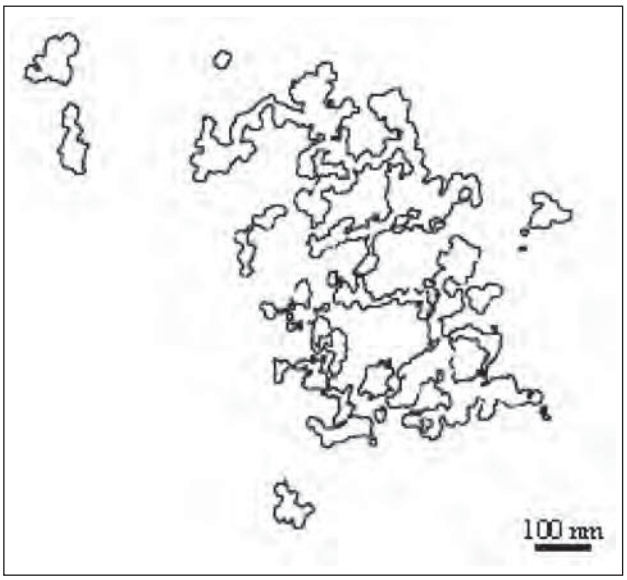

b) Same image after analysis

Figure 3

typical values observed in many rubber compounds that generally are between 1.8 to 2.2 [13]. Images of aggregates taken from dissolved PC are more fibrous-shaped, suggesting that some agglomeration has occurred. The aggregate hetereogeneity index for this latter material is more than twice that of the microtomed PC samples. Close inspection of the unprocessed image shows the presence of the CB black particles.

The distributions of area-equivalent diameter of aggregates for CB in PA6, PC and dissolved PC are shown in Figure 4 a), b) and c), respectively. As seen from Figure 4 a), CB aggregates in this PA6 exhibit a bimodal distribution. The first peak was observed in the range from 60 nm to 80 nm and the second peak in the range of 140 nm to 160 nm. A previous study [15] has also observed bimodal distributions of CB in rubber.

The mean area-equivalent aggregate diameter of PC ranges from 20 to 60 nm. The dissolved PC shows the broadest distribution of area-equivalent diameter from 10-110 nm. This is most likely the result of agglomeration that may have occurred when the PC was put into solution and then precipitated.

Figure 5 shows CB particle diameter histograms in PA6, PC and dissolved PC. The calculated number of the CB particles in PA6, PC and dissolved PC is 626, 749 and 10 130, respectively. The particle diameter for CB in PA6 varies from 20 nm to 50 nm. The particle diameter range for CB in both PC and dissolved PC are smaller and in the range of 5 nm to 20 nm. Both PC-based specimens exhibit the identical particle diameter distributions as expected – the method of preparation of the two PC specimens should not change the primary particle diameter.

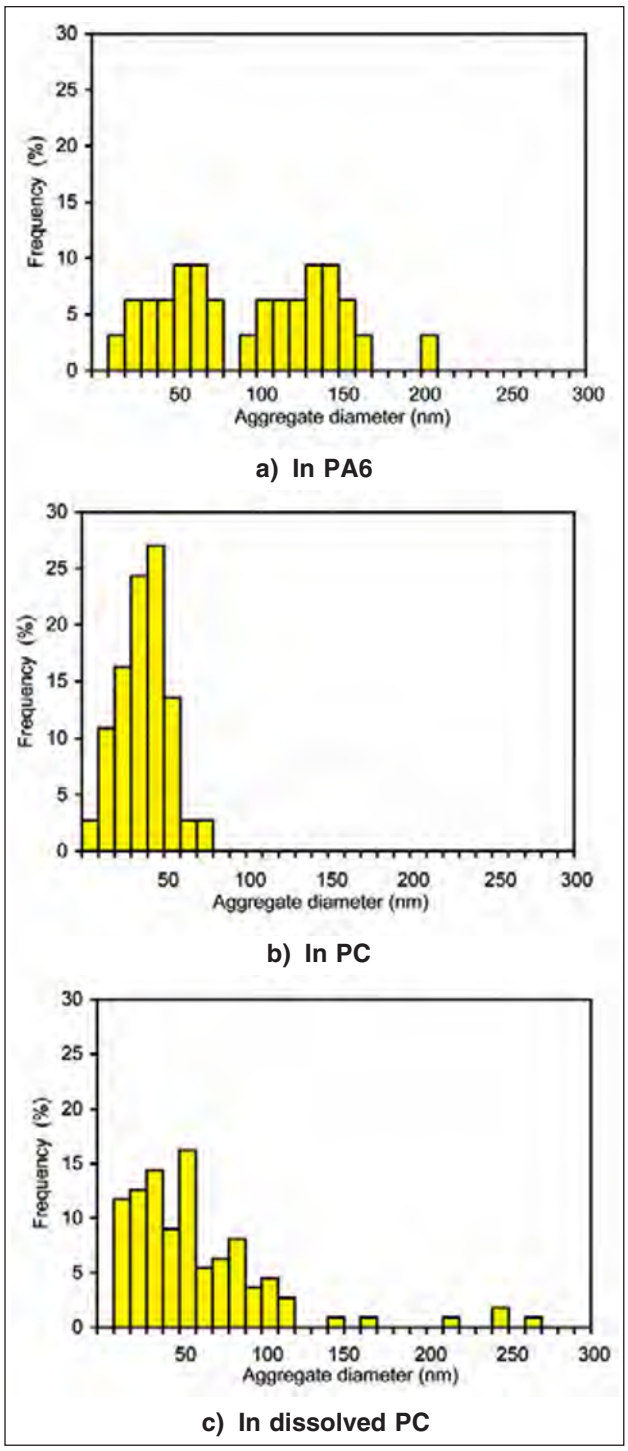

Figure 4 – Distribution of area-equivalent diameter of aggregates for CB

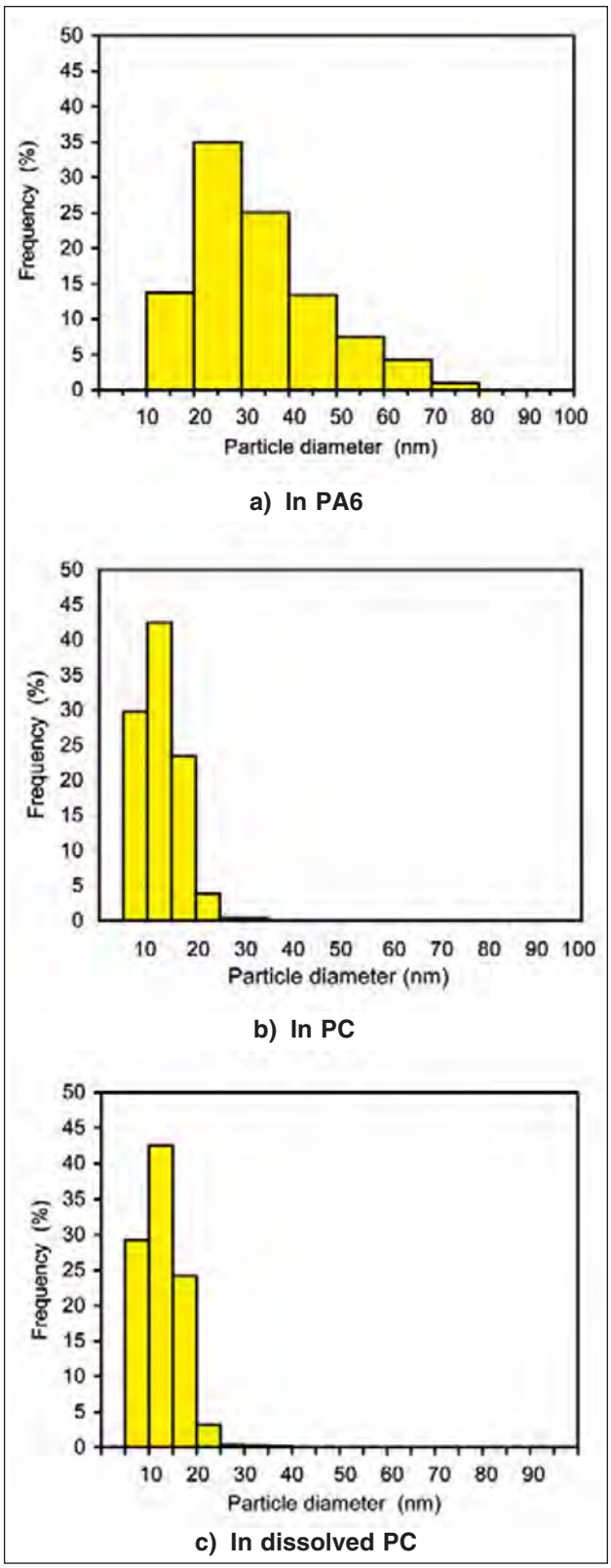

Figure 5 – Distribution of average particle diameter for CB

5.2 Fractal Analysis

The evaluation of the perimeters and areas of CB aggregates leads to the Log P_i versus Log A_i plots shown in Figure 6. The fractal dimensions, which were obtained by calculating the slope of each curve, are used to describe the aggregate shape. The fractal dimension for CB in PA6, PC and dissolved PC are 1.10, 1.18 and 1.36, respectively. The fractal dimensions of PA6 and PC coincide with an ellipsoidal shape, whereas that of dissolved PC indicates that aggregates are more fibrous in nature. The results show a good agreement with the qualitative observation from TEM. These values are also consistent with values of CB in rubber found by others [16, 17].

6 CONCLUSIONS

An image-processing technique has been applied successfully for the quantification of CB size and shape in PA6, PC and dissolved PC using ultramicrotomed sec-

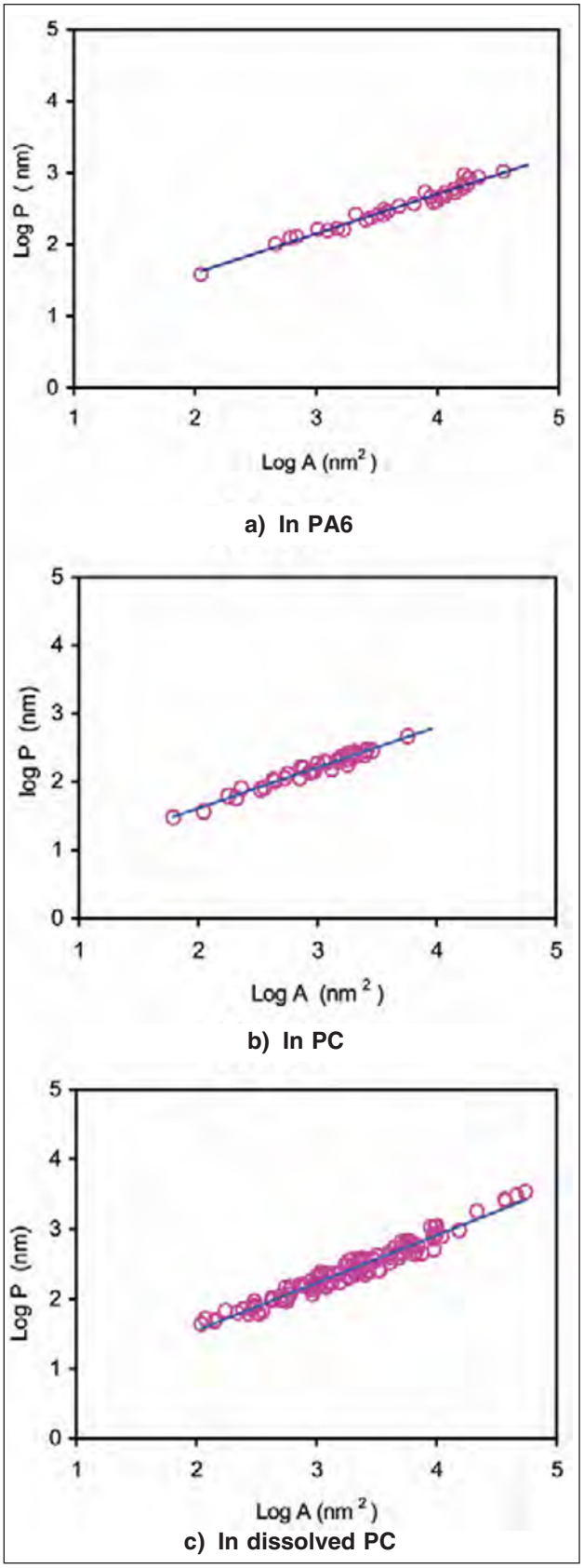

Figure 6 – Log P_i versus Log A_i plot of the microstructure of carbon black

tions and, for PC, dissolved specimens. Both ASTM and fractal analyses were used. CB aggregates in this PA6 exhibited a bimodal size distribution and ellipsoidal shapes. The aggregates in PC were also ellipsoidal but had a normal distribution. Those found in dissolved PC were fibrous in nature, and had a much broader distribution suggesting that the experimental technique may have caused some coalescence. The microtome technique can therefore be used to characterize CB characteristics in thermoplastic polymers used in laser welding. This information will be of use to those modelling this important industrial process.

ACKNOWLEDGEMENTS

The financial support of Jiangsu Government Scholarship for Oversea Study and Excellent Young Teacher Foundation of Soochow University (R2317156) are gratefully acknowledged. In addition the authors would also like to thank AUTO21 Network of Centres of Excellence, Ontario Centres of Excellence – Centre for Materials and Manufacturing, Decoma International and Siemens VDO for their financial support.

REFERENCES

[1] Nonhof C.J.: Polym. Eng. Sci., 1994, 34, 1547.

[2] Atanasov P.A.: Optical Engineering, 1995, 34, 2976.

[3] Leaversuch R.: Plastics Technology, 2002, 48, 56.

[4] Grewell D.A., Benatar A., Park J.B.: Plastics and Composites Welding Handbook, Hanser Gardner Publications, Cincinnate, 2003.

[5] Kagan V.A., Woosman N.M.: J. Reinforced Plastics and Composites, 2004, 23, 351.

[6] Prabhakaran R., Kontopoulou M., Zak G., Bates P.J., Baylis B.: Antec 2004.

[7] Schulz J., Haberstroh E.: Antec 2000, 710.

[8] Chen M., Zak G., Bates P.J.: Antec 2006.

[9] Haberstroh E., Lutzeler R.: J. Polym. Eng., 2001, 21, 119.

[10] Herman F.: Mark (Editor) Carbon Black, Encyclopedia of Polymer Science and Engineering, Vol. 2, Wiley, 1986.

[11] Hess W.M., Chirico V.E., Vegvari P.C.: Elastomerics, January, 24, 1980.

[12] Hess W.M., McDonald G.C.: Rubber Chemistry and Technology, 1983, 56, 892.

[13] Hess W.M., Herd C.R., Sebok E.B., Swartz L.A.: Kautschuk Gummi Kunststoffe, 1994, 47, 5, 328.

[14] Ganesan L., Bhattacharyya P., Bhowmick A.K.: J. of Appl. Polym. Sci., 1995, 56, 1739.

[15] Trifonova-van H.D., Schonherr H., Vancso G.J., Van der D., Noordermeer J.W.M., Janssen P.J.P.: Rubber Chem. Technol., 1999, 72, 862.

[16] Herrmann V., Unseld K., Fuchs H.B.: Colloid Polym. Sci., 2002, 280, 267-276.

[17] Herd C.R., Mcdonald G.C., Hess W.M.: Rubber Chem. Technol., 1992, 65, 107.

[18] ASTM D3849-04, 2004.

[19] Feder J.: Fractals, Plenum, New York, 1988.